Made available through Montana State University's ScholarWorks

A Review on Recent Progress of Biodegradable Magnetic Microrobots for Targeted Therapeutic Delivery: Materials, Structure Designs, and Fabrication Methods

Yang Cao, Kyle Michel, Farzam Alimardani, Yi Wang

ASME © Originally published in Journal of Micro and Nano-Manufacturing

Accessibility Disclaimer:

For a more accessible version of this document, please submit an accessibility request form through the Montana State University Library website.

A Review on Recent Progress of Biodegradable Magnetic Microrobots for Targeted Therapeutic Delivery: Materials, Structure Designs, and Fabrication Methods

Yang Cao[1*], Karen Nunez Michel[1], Farzam Alimardani[2], Yi Wang[2]

1. Mechanical and Industrial Engineering Department, Montana State University, Bozeman, MT 59717
2. Department of Industrial and Systems Engineering, University of Missouri, Columbia, MO 65211

Abstract

Targeted therapeutic delivery employs various technologies to enable precise delivery of therapeutic agents (drugs or cells) to specific areas within the human body. Compared with traditional drug administration routes, targeted therapeutic delivery has higher efficacy and reduced medication dosage and side effects. Soft microscale robotics have demonstrated great potential to precisely deliver drugs to the targeted region for performing designated therapeutic tasks. Microrobots can be actuated by various stimuli, such as heat, light, chemicals, acoustic waves, electric fields, and magnetic fields. Magnetic manipulation is well-suited for biomedical applications, as magnetic fields can safely permeate through organisms in a wide range of frequencies and amplitudes. Therefore, magnetic actuation is one of the most investigated and promising approaches for driving microrobots for targeted therapeutic delivery applications. To realize safe and minimally invasive therapies, biocompatibility and biodegradability are essential for these microrobots, which eliminates any post-treatment endoscopic or surgical removals. In this review, recent research efforts in the area of biodegradable magnetic microrobots used for targeted therapeutic delivery are summarized in terms of their materials, structure designs, and fabrication methods. In the end, remaining challenges and future prospects are discussed.

Keywords: magnetic microrobot, biodegradability, biocompatibility, biomimetics, targeted therapeutic delivery

1 Introduction

Therapeutic delivery applies various methods and technologies to enable the delivery of therapeutic agents (drugs or cells) to specific areas within the human body. In traditional drug delivery systems such as enteral routes (oral, rectal, sublingual) and parenteral routes (intravenous, intramuscular, subcutaneous, intraarterial) [1], the medication is distributed throughout the body via blood circulation. For most therapeutic agents, only a small portion of the medication reaches the area to be affected [2]. Therapeutic cells can also be transplanted to restore or repair damaged biological tissues, also known as tissue engineering. Traditional tissue engineering relies on injection to introduce cells into the body, either into the systemic circulation or directly into the tissue of interest. These methods have shown limited clinical success due to the restricted distribution of the transplanted cells after their introduction into the body [3]. Targeted therapeutic delivery seeks to concentrate the medication or cells in the tissues of interest while reducing the concentration in other areas. Advantages of targeted drug delivery include higher efficacy and reduced medication dosage and side effects.

Targeted therapeutic delivery can be achieved by microscale soft robotics. They can precisely deliver drugs to the targeted region and perform designated therapeutic tasks with minimal incisions. Microrobots can be actuated by various stimuli, such as heat [4], light [5,6], chemicals [7,8], acoustic waves [9], electric fields [10,11], and magnetic fields [12]. Among all these types of microrobots, magnetic microrobots have drawn the widest attention due to the fact that they can be propelled precisely and wirelessly *in vivo* using magnetic fields. Magnetic fields are capable of penetrating most materials and are nearly harmless to human beings [13]. The untethered microrobots can be precisely navigated to hard-to-reach, confined, and delicate inner body sites for various minimally invasive biomedical operations, such as targeted drug delivery [14-18] and cell delivery [19-22]. To ensure safe therapeutic delivery, biocompatibility and biodegradability are essential to the safe deployment of microrobots and noncytotoxic degradation in the human body.

Over the past decade, there has been intense interest in the study of biodegradable magnetic microrobots used to deliver therapeutic agents to targeted areas. This review summarizes the research efforts that have utilized magnetic microrobots for therapeutic delivery applications. Section 2 lists the biodegradable materials commonly used in the fabrication of magnetic microrobots, including polymers and bio-template materials. Note that we focus only on the base structure materials, while interested readers can find more information about the motion-driven functional materials (i.e., magnetic nanoparticles) in references [23-27]. Section 3 focuses on the bioinspired designs and

* Corresponding author: yang.cao1@montana.edu

locomotion mechanisms of magnetic microrobots. Section 4 discusses the commonly used fabrication methods, including two-photon polymerization (2PP), self-assembly synthesis (SAS), bio-templated synthesis (BTS), glancing angle deposition (GLAD), and template-assisted electrochemical deposition (TAED). Section 5 summarizes the existing challenges and future prospects, and Section 6 concludes the article.

2 Biodegradable Materials

The materials used in the fabrication of magnetic microrobots play a critical role in the fabrication process and subsequent applications. In addition to the materials having to be compatible with the manufacturing methods, they also need to be highly biocompatible and biodegradable. The biocompatibility of magnetic microrobots means they can be deployed into the human body without producing adverse effects [28]. Additionally, magnetic microrobots should be biodegradable, which generally refers to the capability of their constructing materials to be degraded by hydrolytic, enzymatic, metabolic, or other biological reactions in the human body without producing cytotoxic byproducts [29-31]. So far, commonly used biodegradable materials in the fabrication of magnetic microrobots include polymers and bio-template materials, whose biodegradation mechanism can be found in references [32,33].

2.1 Polymers

Fabrication of magnetic microrobots usually involves building a three-dimensional (3D) microstructure using a base material, thereafter magnetic nanoparticles and drugs are decorated onto the surface of the robot. When selecting an appropriate base material, several properties of the material need to be carefully considered, such as mechanical properties, biocompatibility, and biodegradability. Currently, the most widely used biodegradable base materials in the fabrication of magnetic microrobots are polymers, such as low molecular weight acrylates, including poly(ethylene glycol) diacrylate (PEGDA) and pentaerythritol triacrylate (PETA) [34-36]. Although their biodegradability has been proved in alkaline conditions, previous evidence has shown substantial cytotoxicity of acrylate monomers and polyacrylic acids resulting from degradation, which are difficult to extract from the human body [37]. Recently, gelatin methacrylate (GelMA) [22,38-41] based magnetic microrobots fabricated by 2PP have gained increasing attention, due to their lower cytotoxicity. Moreover, GelMA can be selectively degraded by collagenase, which is secreted by macrophages, monocytes, synovial cells, and epithelial cells [42]. Other commonly used polymers include hyaluronic acidmethacryloyl (HAMA) [39], polylactic-co-glycolic acid (PLGA) [43-45], polycaprolactone (PCL) [46,47], poly(ethylene glycol) (PEG) [48], N-isopropylacrylamide (NIPAM) [49], and sodium alginate [50]. Table 1 lists the commonly used polymers that have been reported in the fabrication of biodegradable magnetic microrobots. Additional biodegradable materials commonly used in the fabrication of soft robotics can be found in references [12] and [51].

2.2 Bio-template materials

In this paper, bio-template materials are defined as living materials, including cells, bacteria, and fungi, that are directly used as templates to build magnetic microrobots. The importance of bio-template materials is underscored by their similarities to tissues, ensuring compatibility with the human body. Utilizing them in microrobot fabrication brings several advantages, such as easy fabrication procedure, high compatibility, and biodegradability. For instance, mouse macrophage cells exhibit minimal biocompatibility and biodegradation issues and possess innate tumor-infiltration characteristics [13]. *Spirulina platensis* (*S. platensis*) has an inherent helical shape, anti-viral, antibacterial, anti-tumoral, and autofluorescence properties, and its biological composition is naturally degradable [18,52-55]. *Serratia marcescens* (*S. marcescens*) bacteria can be easily cultivated and adhere well to microstructure surfaces, facilitating its integration into bio-hybrid microsystems [56]. Ganoderma lucidum spores offer biodegradability, and possess large hollow cavity and a rough, porous surface that is ideal for drug delivery purposes [57]. However, precise steering control of these heterogeneous systems is still a challenge due to their poor mechanical properties and strong stochastic behaviors during the navigation process. Moreover, a lot of microorganisms cannot be directly applied in *in vivo* applications without genetic modifications [56]. Table 1 lists the bio-template materials that have been reported in the fabrication of magnetic microrobots.

Table 1 Biodegradable materials used in the fabrication of magnetic microrobots

Category	Material	Young's modulus	Biocompatibility	Biodegradability	Fabrication method	State of readiness	References
Polymers	Poly(ethylene glycol)diacrylate (PEGDA)	11–64.4 KPa	Good	Good	2PP	*In vitro*	[34-36,58]
	Pentaerythritol triacrylate (PETA)	1.85–250 GPa	Good	Good	2PP	*In vitro*	[34-36,59,60]
	Gelatin methacryloyl (GelMA)	3–180 KPa	Excellent	Excellent	SAS, 2PP	*In vitro*	[22,38-41,61]
	polylactic-co-glycolic acid (PLGA)	891.2 MPa	Good	Good	SAS, Laser micromachining	*In vitro*	[43-45, 62]
	Poly vinyl alcohol (PVA)	707.9 MPa	Good	Fair	SAS	*In vitro*	[43,63]
	Polycaprolactone (PCL)	343.9–363.4MPa	Fair	Fair	SAS	*In vitro*	[46,47,64]
	Polyethyleneimine (PEI)	3.4–5.6 GPa	Poor	Poor	SAS	*In vitro*	[47,65]
	Poly(ethylene glycol) (PEG)	0.5–4.6 MPa	Fair	Poor	2PP	*In vitro*	[48,66]
	N-isopropylacrylamide (NIPAM)	5–60 KPa	Fair	Fair	Extrusion	*In vitro*	[49,67]
	Sodium alginate	0.1–10 KPa	Good	Good	Extrusion	*In vitro*	[49,50,68]
Bio-template materials	Mouse macrophage cells	90–200 Pa	Unknown	Excellent	BTS	*In vivo*	[13,69]
	Spirulina platensis (*S. platensis*)	Unknown	Good	Excellent	BTS	*In vivo*	[18,52-54]
	Serratia marcescens (*S. Marcescens*)	Unknown	Unknown	Excellent	BTS	*In vitro*	[56]
	Ganoderma lucidum spores	Unknown	Unknown	Excellent	BTS	*In vitro*	[57]

3 Bioinspired Designs and Locomotion Mechanisms

3.1 Bioinspired designs

Besides sphere-shaped [70] (Fig.1 *(g)*) and rod-shaped [71] (Fig.1 *(h)*) magnetic microrobots, bioinspired designs are widely adopted in the development of microscale robotics, which offer better controllability and higher propulsive efficiency [46]. These biomimetic microrobots leverage the advantages of natural mechanical intelligence to achieve highly efficient locomotion with a simple structure, such as bacteria flagella, cilia, fish, scallops, etc. Since the 18th century, biologists have recognized that flagella might be the major propulsion mechanism for a number of microorganisms. However, it was not until the late 19th century that scientists confirmed that the primary means of motion generation in actively propelling microorganisms is through flagella or cilia [72]. The majority of currently reported magnetic microrobots are developed based on these propulsion mechanisms due to the simple structure with efficient locomotion. In addition to the locomotion of microorganisms, the swimming mechanisms of small animals, such as fish and scallops, have also been explored and applied in microrobot propulsion.

Flagella represent one of the most commonly utilized locomotion mechanisms for magnetically actuated microrobots. Flagellar propellers can be categorized into two types with slightly different propulsion mechanisms. One straightforward approach to generate helical propulsion involves rotating a rigid helical "tail" with the assistance of a rotary motor. In 1973, Berg successfully demonstrated that *E. coli* bacteria employ molecular motors to rotate their helical flagella [73]. The swimming method of *E. coli* bacteria is termed "corkscrew" motion, which uses a nonreciprocal motion to achieve a net displacement in low Reynolds number fluids [74]. This mechanism inspired later scientists to develop various flagella-based microrobots. In 2007, Bell et al. [75] first introduced the helical

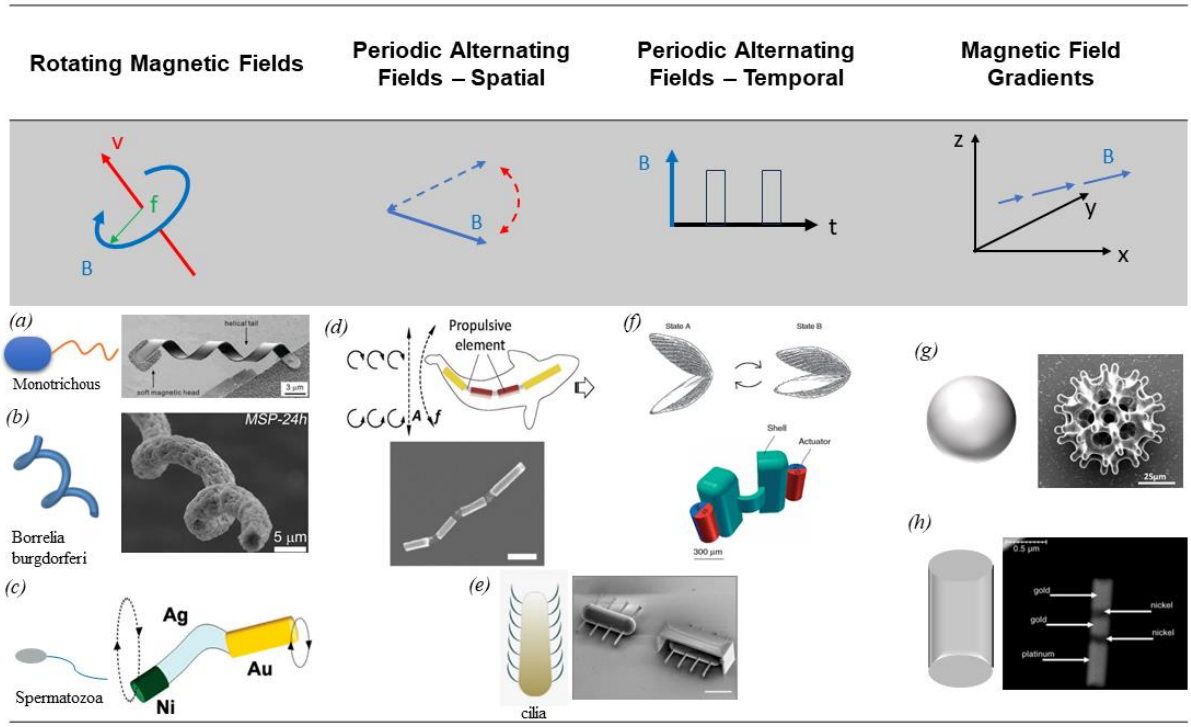


Fig. 1 Bioinspired designs and locomotion mechanism of magnetic microrobots. *(a)* Helical artificial bacterial flagellum propelled by rotating magnetic fields. Reproduced with permission. Copyright 2009 American Chemical Society [*76*]; *(b)* A micro-helical multifunctional magnetite microrobots for imaging-guided therapy. Reproduced with permission. Copyright 2017 American Association for the Advancement of Science [18]; *(c)* A magnetically powered flexible flagellum microrobot. Reproduced under the terms of the cc-by license [87]; *(d)* A fish-like microrobot actuated under an on-off magnetic field. Scale bar: 800 nm. Reproduced with permission. Copyright 2016 Wiley-VCH Verlag GmbH & Co [94]; *(e)* Ciliary microrobots with nonreciprocal magnetic actuation. Scale bar: 100 μm. Reproduced under the terms of the cc-by license [92]; *(f)* 3D model of the 'micro-scallop'. Reproduced under the terms of the cc-by license [97]; *(g)* SEM image of a porous spherical microrobot driven by magnetic field gradients. Reproduced with permission. Copyright 2018 American Association for the Advancement of Science [19]; *(h)* SEM image of 1.5 μm × 400 nm striped metallic rod. Reproduced with permission. Copyright 2005 Wiley-VCH Verlag GmbH & Co [71].

microrobot that mimics *Monotrichous* bacterial propulsion with an artificial bacterial flagellum. The artificial bacterial flagellum comprises a stiff InGaAs/GaAs helical tail connected to a soft magnetic metal "head" for the purpose of actuation, as shown in Fig. 1*(a)* [76]. Subsequently, Zhang et al. [77] conducted additional characterizations and studies of precise motion control of artificial bacterial flagellum-based microrobots. Different head shapes of helical microrobots have also been widely studied, such as square shapes [78,79], circular shapes [75], spherical shapes [80], and cylindrical array shapes [81,82]. Apart from a single artificial bacterial flagellum, microrobots with multiple flagella [83,84] connected to a single magnetic head were also explored by researchers, which mimics the locomotion of *Lophotrichous* or *Amphitrichous* bacteria. One advantage of multiple-flagellum propulsion is that it can provide higher torque and fine-tuned control than a single flagellum. Compared with helical microrobots with a head, microrobots without a head have simpler structures and are easier to fabricate, while they have similar swimming performance [85]. To magnetize helical tail-only microrobots, the microrobots are coated with magnetic particles on the surface or embedded inside the entire body, as shown in Fig. 1*(b)*. Because of the single-helix structure, the microrobot has the advantage of a small contact area with fluids, so it only requires a relatively low magnetic field strength to propel in fluidic environments. In addition, these microrobots can swim inside a fibrous environment, making them promising for *in vivo* applications. Recently, more research has adopted the helical tail-only structure as the microrobot design with various novel functional and biodegradable materials. Moreover, the viscosity and heterogeneity of a dynamic environment, such as blood, may increase operating resistance and reduce motion efficiency. When encountering clots in high-viscosity fluids or becoming trapped by viscous materials, hollow single-helix microrobots could be actuated to create a passage, disperse agglomerates, or eliminate adhesive substances. To address these issues, solid double-helix microrobots with a drill-like head that can maintain motion stability and manipulation efficiency were explored [86], but the research to optimize these novel structures is still at an early stage.

The second type of locomotion mechanism is flexible flagella, exemplified in the case of spermatozoa, which achieve propulsion through their flexible flagella's planar waveform beating. Due to its simple structure, the flexible flagellum can be easily fabricated using a flexible sheet or beam attached to a magnetic head. For example, a flexible nanowire with a gold "head" and nickel "tail" linked by a partially dissolved and weakened silver bridge, can be driven by a rotating magnetic field [87], as shown in Fig. 1*(c)*. Pak et al. [88] also designed a similar microrobot using a flexible nanowire with a nickel head and porous silver tail, which can be propelled under a combination of rotating and gradient magnetic fields. It remains a challenge to fabricate a flexible yet stable structure at microscale. Dreyfus et al. [89] presented another approach to form a flexible flagellum, which used self-assembled magnetic beads to create a flexible tail attached to a blood cell. They found that disrupting the motion symmetry of the traveling wave along the bead chain was achieved by attaching a payload to one end of the chain, which enables the transportation of a single red blood cell.

Another microrobot locomotion mechanism is inspired by cilia, which has shorter, hair-like structures that cover the outside of the cell body. Cilia are among the first natural filaments that have been extensively investigated [90]. They serve not only as a method for propelling microorganisms like the well-known paramecium, but also play a role as stationary fluid transporters, such as aiding in the movement of mucus in our airways [91]. A single cilium exhibits rhythmic beating in two stages: the effective stroke, which straightens and propels a large volume of fluid; and the recovery stroke, which bends and pulls a smaller amount of fluid closer to the cell surface. When cilia are arranged in an array, hydrodynamic interactions cause them to beat out-of-phase, resembling a wave-like motion known as a metachronal wave. The motion generation mechanism of all these slender filaments relies on a combination of drag imbalance acting on a cylindrical element and a nonreciprocal motion. One of the typical ciliary microrobots uses slender beams or rods with etched cilia [92], as shown in Fig. 1*(e)*. Magnetic nanowires, encompassing permanently magnetic thin films, magnetized polymers, and smart material-based magnetized structures, constitute a primary category of artificial cilia [93].

Besides the locomotion mechanisms of microorganisms, the swimming mechanism of small animals, such as fish, has also inspired the design for microrobot propulsion. Fish generate thrust by using their bodies and fins to move forward. To mimic fish swimming, magnetic microrobots use alternating magnetic fields to induce asymmetrical shape deformations, thereby escaping Purcell's "scallop theorem" [74]. For example, Li et al. [94] introduced a fish-like nanoswimmer composed of a gold head segment, two nickel body segments, and a gold caudal fin segment, all connected by three flexible porous silver hinges, as shown in Fig. 1*(d)*. To simplify, two or more rigid segments connected to each other by springs can also achieve undulating motion for magnetic microrobots [35]. For the fish-like microrobot, flexible hinges or tails play a pivotal role in nanowires as they connect the segments and preserve the microrobot's flexibility [95]. Additionally, research has shown that the fish-like microrobot requires a minimum of three segments to move forward smoothly, with optimal performance achieved using four or five segments [96].

Biological microorganisms swim via flagella and cilia that perform nonreciprocal motion to achieve propulsion at low Reynolds numbers in viscous fluids. This symmetry requirement arises from Purcell's scallop theorem,

complicating the actuation schemes needed by microswimmers. However, most biological fluids are non-Newtonian, where the scallop theorem is no longer applicable. It is possible to design microswimmers that move using reciprocal periodic body-shape changes in non-Newtonian fluids. Qiu et al. [97] constructed a single-hinge microswimmer designed to reciprocally open and close its shell body, mimicking scallop motion in non-Newtonian biological fluids, as shown in Fig. 1*(f)*. The opening angle of the micro-scallop robot correlates with the strength of the applied external magnetic field. Despite being limited to reciprocal motion, the micro-scallop robot achieves propulsion in low Reynolds number fluids by employing a time-asymmetric stroke pattern and leveraging the strain rate-dependent viscosity of shear-thickening and shear-thinning fluids. This reciprocal swimming mechanism opens new possibilities for designing microrobots that can be propelled using simple actuation schemes in non-Newtonian biofluids. Interested readers can find more bioinspired microrobot designs in references [72,98] and their locomotion mechanisms in references [99,100].

3.2 Locomotion mechanisms

The basic principle of magnetic actuation involves applying magnetic forces and/or torques to manipulate the magnetized components of a microrobot. To propel a magnetic microrobot, magnetic force (F_m) and/or torque (T_m) can be generated on the microrobot by applying an external magnetic field with a magnetic flux intensity of B, which can be expressed as [101]:

$$T_m = VM \times B \tag{1}$$

$$F_m = V(M \cdot \nabla)B \tag{2}$$

where V is the volume of the magnetic body, and M is magnetization.

Since the magnetization of the magnetic microrobot can be varied across its body geometry, materials, and applied field, an average magnetization would be used by considering the total dipole moment of a magnetic body, which is the product of the magnetic body volume and the average magnetization. According to Eqs. (1) and (2), the magnetic torque is proportional to the magnetic field, which acts to align the magnetization of an object with the field, and the magnetic force is proportional to the gradient of the magnetic field, which is used to actuate the object in the field towards a local maximum. Therefore, magnetic microrobots can be propelled through two primary mechanisms: (a) being rotated by a torque and further propelled through a helical structure or (b) being pulled through a magnetic force.

In order to control magnetic microrobots effectively, magnetic actuation systems can generate various modes of external magnetic fields to enable continuous actuation. Three typical modes of external magnetic fields include:

(1) **Rotating magnetic fields:** These fields involve the continuous rotation of the field vector around an axis, as shown in Fig. 1 (left column). Rotating magnetic fields are often used to actuate helical microrobots and flagella-based microrobots, causing them to rotate around their helical axis with motion occurring perpendicular to the plane of rotation. Compared with microrobots actuated by other types of magnetic fields, microrobots driven by rotating magnetic fields have excellent maneuverability and precise movement performance. According to Huang's [102] research on various artificial microrobots driven by rotating magnetic fields, helical microswimmers were the fastest in high-viscosity fluids due to their dominant corkscrew motion, while flagellar microswimmers exhibited the best motility in low-viscosity fluids. Additionally, larger bodies exhibit greater motility in low-viscosity environments, whereas smaller bodies show higher motility in high-viscosity environments. By leveraging the advantage of rotating magnetic field-driven locomotion, the microrobots can achieve diverse mechanical tasks, such as cargo transport [103,104], assembling [105], etc. In addition, instead of using individual microrobots, cooperative manipulation of microrobot swarms can be accomplished using rotating magnetic fields [104,106]. Even though the rotating magnetic field is easy to generate in a small 3D space, precision control is still challenging due to the nonlinear and distorted magnetic fields. The underlying actuation mechanisms are still unclear, especially for microrobot swarms. In recent years, artificial intelligence has been employed to improve motion control and expand the capabilities of the next-generation microrobots [107]. Future research is expected to concentrate on enhancing magnetic control systems for efficient and precise microrobot manipulation, as well as developing physical and mathematical models to comprehend the control principles influencing their movement under different conditions.

(2) **Periodic alternating magnetic fields:** This category encompasses all temporal alternating magnetic fields apart from rotating fields. These magnetic fields can vary in space (spatially) and/or time (temporally), enabling microrobots to be actuated in different modes for different applications. Most microrobots driven by alternating magnetic fields have a multi-joint or spring structure, which mimics the swimming mechanism of scallops [97] or fish [94], as shown in Fig. 1 (middle two columns). When the magnetic field is active, the bodies are magnetized, leading to mutual attraction. Upon deactivation of the magnetic field, the stored energy in the restoring spring causes the bodies to separate. The on-off cycle of magnetic fields occurs rapidly, enhancing the forward motion of these micro-actuators to be very fast. According to the reported research, Li's fish-like

microrobots can achieve a dimensionless maximum speed (body length / (max speed × frequency)) of 0.63 [94], which is higher than most flagella-driven microrobots. In addition, flexible flagella-like swimmers can also be propelled by field vectors moving up and down in the same plane instead of a magnetic field with temporal on-off cycles [89]. By alternating the magnetic field's direction and frequency, ciliary microrobots can also achieve stroke motion in a fluidic environment with a low Reynolds number. They are powered by the net propulsive force from the beating locomotion of cilia, and on−off fields with designated angles can precisely control their position and orientation. Ghanbari et al. [93] proposed an artificial cilium that can reach a maximum speed of 4,500 μm/s with an efficiency of 40%. Despite the efficiency demonstrated by numerous studies on alternating magnetic field-driven microrobots in low Reynolds number fluids, challenges remain for their *in vivo* applications, especially within flowing blood vessels. Moving forward, investigating the interaction between microrobots and their surrounding fluids is crucial to enhancing motion capability and efficiency for *in vivo* applications.

(3) **Magnetic field gradients:** In this mode, the robot aligns itself with the direction of the magnetic field and moves along the field gradient, as shown in Fig.1 (right column), which may not necessarily coincide with the orientation of the field. The microrobots driven by magnetic field gradients are normally designed with simple symmetric structures [19], such as spherical (Fig. 1 *(g)*) and cylindrical structures (Fig. 1 *(h)*), facilitating ease of miniaturization and low manufacturing cost. One consideration is that these simple structures experience little surface friction [108], therefore enabling higher motion efficiency. The elliptical body is close to the minimum drag shape at low Reynolds numbers [109,110]. Compared with microrobots actuated by other types of magnetic fields, the microrobots driven by magnetic field gradients are more sensitive to the magnitude of the field gradient. While a large magnetic field gradient can propel microrobots at high speeds, their mobility will be greatly reduced by a small field gradient. Due to the simple driving mode, most field gradient-driven microrobots are used for cargo transport and drug delivery within a 1D or 2D magnetic gradient system [111]. In addition to controlling individual microrobots, magnetic field gradients can also be harnessed for the manipulation of microrobot swarms [112]. While most microrobots are driven by 1D or 2D magnetic gradients, utilizing a 3D magnetic gradient enables more complex and precise locomotion in 3D spaces. This advancement is particularly beneficial for *in vivo* medical applications, such as the navigation of intraocular microrobots [113]. One advanced 3D electromagnetic system is the OctoMag configuration, which utilizes eight magnets to provide precise navigation with up to five degrees of freedom (5-DOF, 3-DOF position and 2-DOF orientation) and even 6-DOF [113-115]. However, full pose control, including both position and orientation, is still challenging currently for untethered magnetic devices, limiting the adoption of magnetically driven microrobots for non-invasive medical applications.

4 Fabrication Methods

In this section, we summarized the five most commonly used techniques in fabricating magnetic microrobots or nanorobots, which include two-photon polymerization (2PP), self-assembly synthesis (SAS), bio-templated synthesis (BTS), glancing angle deposition (GLAD), and template-assisted electrochemical deposition (TAED). A comparison of these five techniques is presented in Table 2. Interested readers may refer to the references for other fabrication methods, such as electrospinning [116-118] and photolithography [78,102,119].

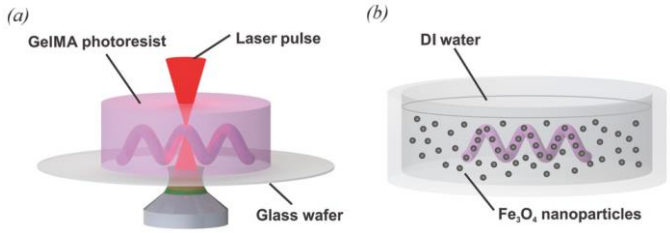


Fig. 2 Schematic of using 2PP to fabricate magnetic microrobots. *(a)* 2PP is used to print GelMA helical microstructures; *(b)* The printed structures are decorated with magnetic nanoparticles by incubating in a water suspension of Fe_3O_4 nanoparticles. Reproduced with permission. Copyright 2018 WILEY-VCH Verlag GmbH & Co [41].

4.1 Two-photon polymerization (2PP)

To date, photopolymerization-based 3D printing, especially 2PP [86,120], is the most widely used method for fabricating helical magnetic microrobots. 2PP, also known as direct laser writing, is a photopolymerization process based on the simultaneous absorption of two photons in a photocurable material. Compared with one-photon absorption, two-photon absorption can significantly reduce the absorption cross-section, thus offering the highest resolution currently available in 3D printing (~100 nm) [121]. As shown in Fig. 2, the typical fabrication procedure involves photopolymerization of photocurable hydrogels to create the microrobot structure, then magnetic particles and medications are decorated on the outside surface of the microstructure by incubating in an aqueous suspension of magnetite nanoparticles [38]. This fabrication method relies on photopolymerization, which largely limits the applicable materials to photocurable hydrogels, such as GelMA [38-41,86], PEGDA [34,36], and methacrylamide chitosan (ChMA) [122]. Moreover, drugs and cells are usually coated onto the outside surface of the microrobot. This not only limits the amount of therapeutic agents that the microrobot can carry, but also inevitably causes drug loss before they reach the desired location.

4.2 Self-assembly synthesis (SAS)

A common type of magnetic microrobot has a spherical structure. The locomotion of spherical magnetic microrobots either relies on rotation on a surface [46,123], or direct magnetic attraction [43,48]. Due to the simple structure, they can be fabricated by a relatively simple self-assembly synthesis method. Generally, hydrogel is used as the base material, then magnetic nanoparticles and therapeutic agents are encapsulated into the base material through emulsion, stirring, sonication, etc. Fig. 3 shows the fabrication process of a water-immiscible (MAWI) coacervate magnetic microrobot derived from the supramolecular interaction-driven self-assembly of inorganic-organic hybrid core-shell nanoparticles [48]. It starts with a core-shell nanostructure that has a superparamagnetic iron oxide nanoparticle (SPION) core and PEG shell, and then WAWI coacervates are assembled through water dialysis. The self-assembly synthesis method is simpler and more cost-effective than other fabrication methods, which is suitable for mass production. Other than that, a unique characteristic of magnetic microrobots fabricated by this method is that the therapy agents are encapsulated in the structural material, so the drug release rate can be controlled as the shell material degrades. For instance, Pacheco et al. [46] fabricated magnetic microrobots with enzymatically encoded drug release. The microrobot is chemically programmed in such a way that the polymer layer is degraded by the enzymatic activity of lipase, which is overexpressed in pancreatic cancer cells. This causes degradation of the microrobot's polymer layer, thus destructing the robot and releasing the anticancer drug in a controlled manner.

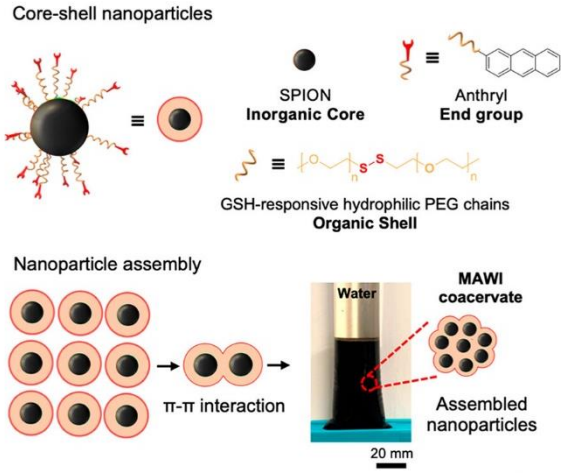


Fig. 3 Inorganic−organic hybrid core−shell nanoparticles assembled into the magnetically actuatable and water-immiscible (MAWI) coacervate via fluid−fluid phase separation. Reproduced with permission. Copyright 2023 American Chemical Society [48].

4.3 Bio-templated synthesis (BTS)

Microorganisms such as microalga and bacteria have evolved billions of years and possess diverse microstructures and biological properties. Engineering microorganisms as templates to build magnetic microrobots seems a very

promising option [124,125]. The magnetization of biological entities with certain specifications could allow the fabrication of magnetic microrobots that incorporate the morphological and functional features of a biological matrix. The fabricated bio-templated microrobots are composed of degradable biomaterials and magnetic functional particles. Furthermore, the inherited functionalities could be tailored for specific applications. One representative is *S. platensis*, which has an inherent helical structure that can be directly used for corkscrew navigation. Yan et al. [18,54] and Xie et al. [53] have done some pioneering research work in this area. As shown in Fig. 4, a hollow helical microswimmer possessing an outer shell aggregated by mesoporous spindle-like magnetite nanoparticles and a helical-shaped inner cavity was fabricated. The fabrication is a cost-effective mass-production process of bio-templated synthesis using the helical microorganism *S. platensis*. Specifically, magnetite precursors are first deposited on the surface of *S. platensis* through a magnetite precursor solution ($FeCl_2$–$FeCl_3$), followed by annealing treatment and reduction processing to remove the *S. platensis* core and eventually obtain nanostructured porous hollow magnetic microhelices. A similar method has also proved feasible for magnetizing other microalgae species, for example, *Tetraselmis subcordiformis* and *Chlamydomonas reinhardtii* [18]. The innate properties of these microalgae allowed *in vivo* fluorescence imaging without any surface modifications. Another representative work was done by Yasa et al. [126]. They reported a biocompatible biohybrid microswimmer powered by a unicellular freshwater green microalga, *Chlamydomonas reinhardtii*. Polyelectrolyte-functionalized magnetic spherical cargoes were attached to the surface of the microalgae via noncovalent interactions. As a proof-of-concept demonstration, fluorescent isothiocyanate-dextran molecules were effectively delivered to mammalian cells using the biohybrid algal microswimmers. Other than microalga, macrophage cells [13] and *Serratia marcescens* bacteria cells [56] have also been used as building templates for magnetic microrobots. Using microorganisms as the building templates for magnetic microrobots is still an evolving area. Several essential aspects remain to be explored in future work, especially navigation capability, therapeutic agent loading and release, and potential host responses in *in vivo* testing.

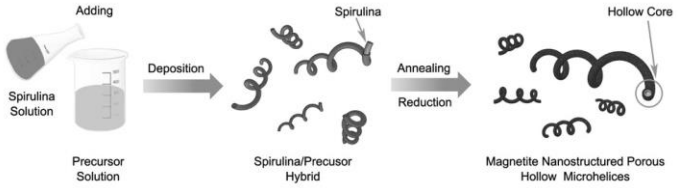


Fig. 4 Schematic of using *S. platensis* as bio-templates to fabricate helical magnetic microrobots. Reproduced with permission. Copyright 2015 WILEY-VCH Verlag GmbH & Co [54].

4.4 Glancing angle deposition (GLAD)

GLAD is a thin film deposition technique that is primarily based on the electron-beam evaporation process. In traditional thin film deposition, a stream of vapor-phase atoms strikes a perpendicular substrate. In GLAD, the substrate is tilted from the perpendicular direction of the vapor flux, so that the atoms strike the substrate obliquely. Furthermore, the substrate can be rotated to control the growth of the deposited film [127,128]. GLAD has proven to be an effective approach to mass produce nanoscale helical magnetic microrobots and nanorobots [129-132]. As shown in Fig. 5, a silicon wafer is first covered with a seed layer, such as a monolayer of silica beads. The helical structures are then grown on the seed layer using GLAD. Magnetization of the helical structures can be done subsequently by coating a thin layer of ferromagnetic materials (e.g., cobalt, iron, nickel) through thermal evaporation or sputter coating. The helical magnetic microrobots are then removed from the substrate by sonication. Ghosh et al. [80] reported the fabrication of helical magnetic nanorobots using GLAD as well as the navigation of them to achieve micrometer level precision using homogeneous magnetic fields. Kadiri et al. [129] fabricated Fe-Pt co-deposited helical magnetic nanorobots that have high biocompatibility, and low cytotoxicity and magnetic remanence. The magnetic nanorobots were successfully demonstrated for magnetic transfection in lung carcinoma cells. To overcome the difficulty of navigation of magnetic micropropellers in mucin gels, Walker et al. [130] developed urease-immobilized magnetic micropropellers by GLAD. The micropropeller was inspired by the bacterium *Helicobacter pylori* that can penetrate through gastric mucus by producing the enzyme urease to locally change the pH and consequently liquefy the mucus. Wu et al. [131] used GALD to fabricate magnetic micropropellers that could penetrate the vitreous body of the eye and reach the retina. The micropropellers were functionalized with perfluorocarbon coating that minimizes the interaction of the micropropellers with biopolymers. An obvious advantage of GLAD is that it can mass produce nanoscale magnetic microrobots that are suitable for cell-level therapeutic and genetic

applications. However, only certain materials can be used by GLAD, such as metals and silica, some of which are not biodegradable. Another major issue encountered by magnetic nanorobots fabricated by GLAD is thermal noise or Brownian motion during navigation. Magnetic microrobots fabricated by GLAD typically have a length of around 1 μm, while researchers have pointed out that magnetic robots must have a minimum length of 900 nm in water, otherwise Brownian motion will dominate their navigation [132,133].

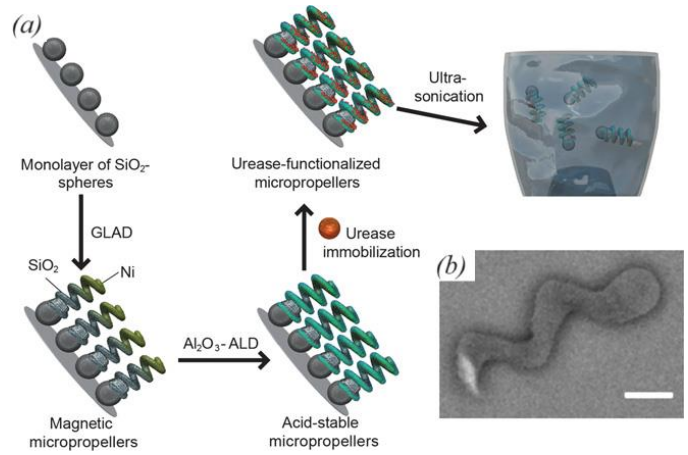


Fig. 5 Fabrication of helical urease-immobilized magnetic nanorobots using GLAD. *(a)* Schematic of the fabrication process; *(b)* SEM image of a magnetic nanorobot, scale bar = 500 nm. Reproduced with permission. Copyright 2015 American Association for the Advancement of Science [130].

4.5 Template-assisted electrochemical deposition (TAED)

TAED is capable of fabricating various nanostructures by using a nanoscale template to confine the chemical or physical reaction to a specific position. Park and his team [134] reported a Cu-Pd co-deposition method to fabricate Pb nanosprings. The fabrication process starts with an anodic aluminum oxide (AAO) template with highly ordered nanopores. The simultaneous electrochemical deposition of Cu and Pd leads to the growth of homogeneous Pd-Cu nanorods. The surface of these nanorods exhibits a periodical distribution of Pb and Cu in a helical pattern, while the core material is Cu. The AAO template and Cu can be selectively etched away in a sodium hydroxide solution and nitric acid solution, respectively, resulting in Pb nanosprings. The magnetization of Pb nanosprings can be achieved by coating a thin layer of Ni with vapor deposition. The diameter, length, and spiral pitch of the magnetic nanorobots

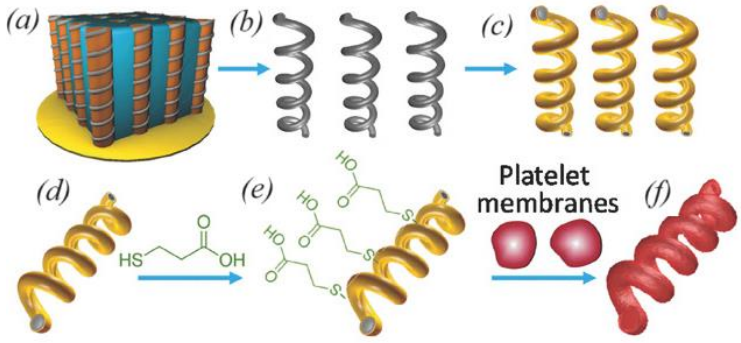


Fig. 6 Fabrication of platelet-camouflaged magnetic nanorobots: *(a)* Pd/Cu co-electrochemical deposition in a polycarbonate template; *(b)* Etching of Cu and release of the helical Pd nanostructures; *(c)* Deposition of Ni/Au bilayer on the Pd helical nanostructure; *(d)* Collection of the helical nanostructures; *(e)* Modification of the bare helical nanomotor surface with 3-mercaptopropionic acid (MPA); *(f)* Fusion of platelet-membrane-derived vesicles to the MPA-modified surface of the helical nanorobot. Reproduced with permission. Copyright 2017 WILEY-VCH Verlag GmbH & Co [137].

can be readily changed by using a template with different pore sizes, electrodeposition parameters, and composition of the plating solution, respectively [135]. This method has been used as an effective approach to fabricate helical magnetic nanorobots [135-137]. For instance, Hoop et al. [136] used TAED to fabricate helical magnetic nanorobots for direct-contact bacterial killing. In addition to a Ni coating for magnetic manipulation, a layer of Ag was also vapor deposited to utilize its antibacterial properties. The efficiency of the magnetic nanorobots was tested in the treatment of *E. coli* and *Staphylococcus aureus*. As shown in Fig. 6, Li et al. [137] reported platelet-camouflaged magnetic nanorobots that could bind to toxins and platelet-adhering pathogens, such as Shiga toxin and *Staphylococcus aureus* bacteria. The helical magnetic nanorobots were fabricated by TAED and coated with the plasma membrane of human platelets, which enabled the nanorobots efficient biofouling resistance and biological binding functions. Other than helical magnetic nanorobots, TAED can also be used to fabricate cylindrical [138-140], tubular [141], and chain-shaped magnetic nanorobots [94,142-144,] in a similar way.

Table 2 Comparisons of commonly used methods to fabricate magnetic microrobots

	Pros	Cons
2PP	• Capable of fabricating highly complex and consistent microscale 3D structures • High yield rate	• Expensive equipment • Limited selection of materials (photocurable hydrogels and resins)
SAS	• Simple process • Cheap equipment • Capable of mass production	• Limited structure complexity (generally spheres) • Structure inconsistency • Low yield rate
BTS	• High biocompatibility and biodegradability • Cheap equipment • Capable of mass production	• Poor mechanical properties • Structure inconsistency • Stochasticity in navigation • Low yield rate
GLAD	• Nanoscale resolution • Simple process • Cheap equipment • Capable of mass production	• Limited selection of materials (usually metals, silica) • Thermal noise
TAED	• Nanoscale resolution • Simple process • Cheap equipment • Capable of mass production	• Limited selection of materials (mainly metals) • Thermal noise

5 Existing Challenges and Future Prospects

Despite the fact that various bioinspired structures have been proposed for magnetic microrobots, the fabrication of biocompatible and biodegradable magnetic microrobots that are safe for clinical applications remains a challenge. First, hydrogels are currently the most commonly used materials in the fabrication of magnetic microrobots. They are biocompatible but generally not completely biodegradable, or upon degradation, they generate cytotoxic products that are difficult to excrete from the human body [37]. Meanwhile, due to their poor mechanical properties, other additives that have lower biodegradability are usually added in the fabrication process. Bio-template materials seem promising due to their high biocompatibility and biodegradability. However, precise steering control of bio-template material-based microrobots is still a challenge due to their poor mechanical properties and strong stochastic behaviors during the navigation process [32,54,55]. Secondly, the fabrication technique is still a bottleneck. 2PP, GLAD, and TAED have a submicron resolution to fabricate complex microstructures, but they have a very limited selection of available materials and limited drug-loading capabilities. SAS is a cost-effective mass production approach, while the structure design is generally limited to microspheres [46,48]. BTS seems very promising, but the consistency, yield rate, and maneuverability are still low, and their biocompatibility needs to be further verified in *in vivo* testing.

There exists a gap between the potential and the current state of biodegradable magnetic microrobots. Up to this point, most research in this field has been focused on microrobot fabrication and *in vitro* testing, but real-world applications still need to be addressed. To bridge this gap, cost-effective, highly consistent, mass-producible

microrobots that have precise navigation and controllable drug release capabilities are needed. More research needs to be done in the following areas:

1) Materials with high biocompatibility and biodegradability and appropriate mechanical properties;
2) Motion dynamics analysis and structure optimization of bioinspired magnetic microrobot designs;
3) Use of machine vision and artificial intelligence techniques to realize precise and intelligent navigation;
4) Controlled degradation and therapeutic release;
5) Deployment and cooperative control of magnetic microrobot swarms.

6 Conclusions

In this review, recent advances in magnetic microrobots are discussed in terms of their materials, structure designs, and fabrication methods. A variety of hydrogels and bio-template materials have shown great potential for use in the fabrication of biodegradable magnetic microrobots due to their high biocompatibility and biodegradability. Besides regular geometrical shapes, the structure designs of most magnetic microrobots are inspired by microorganisms or small animals, such as bacterial flagella, cilia, fish, scallops, etc. We also summarized how these bioinspired designs can be actuated by different locomotion mechanisms, including rotating magnetic fields, periodic magnetic fields, and magnetic field gradients. Five commonly used methods in the fabrication of magnetic microrobots, including 2PP, SAS, BTS, GLAD, and TAED, are discussed in detail. Finally, we present the existing challenges and future research prospects in this area.

References

[1] Kim J., De Jesus O., 2023, "Medication Routes of Administration," StatPearls Publishing, https://www.ncbi.nlm.nih.gov/books/NBK568677/

[2] Trafton A., 2009, "Tumors targeted using tiny gold particles," MIT Tech Talk **53**, pp. 4–4.

[3] Mooney D. J., and Vandenburgh H., 2008, "Cell delivery mechanisms for tissue repair," Cell Stem Cell, **2**(3), pp. 205–213.

[4] Go, G., Nguyen V. D., Jin Z., Park J. O., and Park S., 2018, "A thermo-electromagnetically actuated microrobot for the targeted transport of therapeutic agents," Int. J. Control Autom. Syst., **16**, pp. 1341–1354.

[5] Debata S., Kherani N. A., Panda S. K., and Singh D. P., 2022, "Light-driven microrobots: capture and transport of bacteria and microparticles in a fluid medium," J. Mater. Chem. B, **10**(40), pp. 8235–8243.

[6] Palima D., and Glückstad J., 2013, "Gearing up for optical microrobotics: micromanipulation and actuation of synthetic microstructures by optical forces," Laser Photon. Rev., **7**(4), pp. 478–494.

[7] Gao W., Dong R., Thamphiwatana S., Li J., Gao W., Zhang L., and Wang J., 2015, "Artificial micromotors in the mouse's stomach: A step toward in vivo use of synthetic motors," ACS Nano, **9**(1), pp. 117–123.

[8] Solovev A. A., Mei Y., Ureña E. B., Huang G., and Schmidt O. G., 2009, "Catalytic microtubular jet engines self-propelled by accumulated gas bubbles," Small, **5**(14), pp. 1688–1692.

[9] Aghakhani A., Yasa O., Wrede P., and Sitti M., 2020, "Acoustically powered surface-slipping mobile microrobots," Proc. Natl. Acad. Sci., **117**(7), pp. 3469–3477.

[10] Guo S., Ge Y., Li L., and Liu S., 2006, "Underwater swimming micro robot using IPMC actuator," 2006, Int. Conf. Mechatron. Autom., pp. 249–254.

[11] Tyagi M., Spinks G. M., and Jager E. W., 2021, "3D printing microactuators for soft microrobots," Soft Robot., **8**(1), pp. 19–27.

[12] Llacer-Wintle J., Rivas-Dapena A., Chen X. Z., Pellicer E., Nelson B. J., Puigmartí-Luis J., and Pané S., 2021, "Biodegradable small-scale swimmers for biomedical applications," Adv. Mater., **33**(42), p. 2102049.

[13] Feng Y., Feng L., Dai Y., Bai X., Zhang C., Chen Y., and Arai F., 2020, "A novel and controllable cell-based microrobot in real vascular network for target tumor therapy," 2020 IEEE/RSJ International Conference on Intelligent Robots and Systems (IROS), pp. 2828–2833.

[14] Lee, H., Kim, D. I., Kwon, S. H., and Park, S., 2021, "Magnetically actuated drug delivery helical microrobot with magnetic nanoparticle retrieval ability," ACS Appl. Mater. Interfaces, **13**(17), pp. 19633–19647.

[15] Nguyen, K. T., Go, G., Jin, Z., Darmawan, B. A., Yoo, A., Kim, S., Nan, M., Lee, S. B., Kang, B., Kim, C. S., Li, H., Bang, D., Park, J. O., and Choi, E., 2021, "A magnetically guided self-rolled microrobot for targeted drug delivery, real-time X-Ray imaging, and microrobot retrieval," Adv. Healthc. Mater., **10**(6), p. 2001681.

[16] Peyer, K. E., Tottori, S., Qiu, F., Zhang, L., and Nelson, B. J., 2013, "Magnetic helical micromachines," Chem. Eur. J., **19**(1), pp. 28–38.

[17] Jang, D., Jeong, J., Song, H., and Chung, S. K., 2019, "Targeted drug delivery technology using untethered microrobots: A review," J. Micromech. Microeng., **29**(5), p. 053002.
[18] Yan, X., Zhou, Q., Vincent, M., Deng, Y., Yu, J., Xu, J., Xu, T., Tang, T., Bian, L., Wang, Y. X. J., Kostarelos, K., and Zhang, L., 2017, "Multifunctional biohybrid magnetite microrobots for imaging-guided therapy," Sci. Robot., **2**(12), p. eaaq1155.
[19] Li, J., Li, X., Luo, T., Wang, R., Liu, C., Chen, S., Li, D., Yue, J., Cheng, S. H., and Sun, D., 2018, "Development of a magnetic microrobot for carrying and delivering targeted cells," Sci. Robot., **3**(19), p. eaat8829.
[20] Kim, S., Qiu, F., Kim, S., Ghanbari, A., Moon, C., Zhang, L., Nelson, B. J., and Choi, H., 2013, "Fabrication and characterization of magnetic microrobots for three-dimensional cell culture and targeted transportation," Adv. Mater., **25**(41), pp. 5863–5868.
[21] Yasa, I. C., Tabak, A. F., Yasa, O., Ceylan, H., and Sitti, M., 2019, "3D-Printed microrobotic transporters with recapitulated stem cell niche for programmable and active cell delivery," Adv. Funct. Mater., **29**(17), p. 1808992.
[22] Noh, S., Jeon, S., Kim, E., Oh, U., Park, D., Park, S. H., Kim, S. W., Pané, S., Nelson, B. J., Kim, J., and Choi, H., 2022, "A biodegradable magnetic microrobot based on gelatin methacrylate for precise delivery of stem cells with mass production capability," Small, **18**(25), p. 2107888.
[23] Colombo, M., Carregal-Romero, S., Casula, M. F., Gutiérrez, L., Morales, M. P., Böhm, I. B., Heverhagen, J. T., Prosperi, D., and Parak, W. J., 2012, "Biological applications of magnetic nanoparticles," Chem. Soc. Rev., **41**(11), pp. 4306–4334.
[24] Duguet, E., Vasseur, S., Mornet, S., and Devoisselle, J. M., 2006, "Magnetic nanoparticles and their applications in medicine," Nanomedicine, **1**(2), pp. 157–168.
[25] Lu, A. H., Salabas, E. E., and Schüth, F., 2007, "Magnetic nanoparticles: synthesis, protection, functionalization, and application," Angew. Chem. Int. Ed. Engl., **46**(8), pp. 1222–1244.
[26] Fuentes, O. P., Trujillo, D. M., Sánchez, M. E., Abrego-Perez, A. L., Osma, J. F., and Cruz, J. C., 2024, "Embracing sustainability in the industry: a study of environmental, economic, and exergetic performances in large-scale production of magnetite nanoparticles," ACS Sustain. Chem. Eng., **12**(2), pp. 760–772.
[27] Guillén-Pacheco, A., Ardila, Y., Peñaranda, P. A., Bejarano, M., Rivas, R., Osma, J. F., and Akle, V., 2024, "Low toxicity of magnetite-based modified bionanocomposites with potential application for wastewater treatment: Evaluation in a zebrafish animal model," Chemosphere, **358**, p. 142081.
[28] Vert, M., Doi, Y., Hellwich, K. H., Hess, M., Hodge, P., Kubisa, P., Rinaudo, M., and Schué, F., 2012, "Terminology for biorelated polymers and applications (IUPAC Recommendations 2012)," Pure. Appl. Chem., **84**(2), pp. 377–410.
[29] Huang, H., Dong, C., Feng, W., Wang, Y., Huang, B., and Chen, Y., 2022, "Biomedical engineering of two-dimensional MXenes," Adv. Drug Deliv. Rev., **184**, p. 114178.
[30] Li, C., Guo, C., Fitzpatrick, V., Ibrahim, A., Zwierstra, M. J., Hanna, P., Lechtig, A., Nazarian, A., Lin S. J., and Kaplan, D. L., 2020, "Design of biodegradable, implantable devices towards clinical translation," Nat. Rev. Mater., **5**(1), pp. 61–81.
[31] Ye, M., Zhou, Y., Zhao, H., Wang, Z., Nelson, B. J., and Wang, X., 2023, "A review of soft microrobots: Material, fabrication, and actuation," Adv. Intell. Syst., **5**(11), p. 2300311.
[32] Li, J., and Yu, J., 2023, "Biodegradable microrobots and their biomedical applications: A review," Nanomaterials, **13**(10), p. 1590.
[33] Hutmacher, D. W., Goh, J. C. H., and Teoh, S. H., 2001, "An introduction to biodegradable materials for tissue engineering applications," Ann. Acad. Med. Singap., **30**(2), pp. 183–191.
[34] Park J., Jin C., Lee S., Kim J. Y., and Choi H., 2019, "Magnetically actuated degradable microrobots for actively controlled drug release and hyperthermia therapy," Adv. Healthc. Mater., **8**(16), p. 1900213.
[35] Sun H. C. M., Liao P., Wei T., Zhang L., and Sun D., 2020, "Magnetically powered biodegradable microswimmers" Micromachines, **11**(4), p. 404.
[36] Peters C., Hoop M., Pané S., Nelson B. J., and Hierold C., 2016, "Degradable magnetic composites for minimally invasive interventions: Device fabrication, targeted drug delivery, and cytotoxicity tests," Adv. Mater., **28**(3), pp. 533–538.
[37] Heller C., Schwentenwein M., Russmueller G., Varga F., Stampfl J., and Liska R., 2009, "Vinyl esters: low cytotoxicity monomers for the fabrication of biocompatible 3D scaffolds by lithography based additive manufacturing," J. Polym. Sci. A Polym. Chem., **47**(24), pp. 6941–6954.
[38] Dong M., Wang X., Chen X. Z., Mushtaq F., Deng S., Zhu C., Torlakcik H., Terzopoulou A., Qin X. H., Xiao X., Puigmartí-Luis J., Choi H., Pêgo A. P., Shen Q. D., Nelson B., and Pané S., 2020, "3D-printed soft

magnetoelectric microswimmers for delivery and differentiation of neuron-like cells," Adv. Funct. Mater., **30**(17), p. 1910323.
[39] Hou Y., Wang H., Zhong S., Qiu Y., Shi Q., Sun T., Huang Q., and Fukuda T., 2022, "Design and control of a surface-dimple-optimized helical microdrill for motions in high-viscosity fluids," IEEE ASME Trans. Mechatron., **28**(1), pp. 429–439.
[40] Terzopoulou A., Wang X., Chen X. Z., Palacios-Corella M., Pujante C., Herrero-Martín J., Qin X. H., Sort J., DeMello A. J., Nelson B. J., Puigmartí-Luis J., and Pané S., 2020, "Biodegradable metal–organic framework-based microrobots (MOFBOTs)," Adv. Healthc. Mater., **9**(20), p. 2001031.
[41] Wang X., Qin X. H., Hu C., Terzopoulou A., Chen X. Z., Huang T. Y., Maniura-Weber K., Salvador Pané S., and Nelson B., 2018, "3D printed enzymatically biodegradable soft helical microswimmers," Adv. Funct. Mater., **28**(45), p. 1804107.
[42] Vaes G., 1980, "Cell-to-cell interactions in the secretion of enzymes of connective-tissue breakdown, collagenase and proteoglycan-degrading neutral proteases-a review," Agents Actions, **10**(6), p. 474.
[43] Kim D., Lee H., Kwon S., Choi H., and Park S., 2019, "Magnetic nano-particles retrievable biodegradable hydrogel microrobot," Sens. Actuators B Chem., **289**, pp. 65–77.
[44] Kim J., Jeon S., Lee J., Lee S., Lee J., Jeon B. O., Jang J., and Choi H., 2018, "A simple and rapid fabrication method for biodegradable drug-encapsulating microrobots using laser micromachining, and characterization thereof," Sens. Actuators B Chem., **266**, pp. 276–287.
[45] Zahn D., Weidner A., Saatchi K., Häfeli U. O., Dutz S., 2019, "Biodegradable magnetic microspheres for drug targeting, temperature controlled drug release, and hyperthermia," Curr. Dir. Biomed. Eng., **5**(1), pp. 161–164.
[46] Yang R., Zhu S., Zhang L., Niu F., and Liu S., 2021, "Magnetic microswimmers with infrared-induced shape transformation," Micro Nano Lett., **16**(12), pp. 582–590.
[47] Pacheco M., Mayorga-Martinez C., Viktorova J., Ruml T., Escarpa A., and Pumera M., 2022, "Microrobotic carrier with enzymatically encoded drug release in the presence of pancreatic cancer cells via programmed self-destruction," Appl. Mater. Today, **27**, p. 101494.
[48] Zhao P., Qu F., Fu H., Zhao J., Guo J., Xu J., Ho Y. P., Chan M. L., and Bian L., 2023, "Water-immiscible coacervate as a liquid magnetic robot for intravascular navigation," J. Am. Chem. Soc., **145**(6), pp. 3312–3317.
[49] Lee H., Choi H., and Park S., 2018, "Preliminary study on alginate/NIPAM hydrogel-based soft microrobot for controlled drug delivery using electromagnetic actuation and near-infrared stimulus," Biomed. Microdevices., **20**, p. 103.
[50] Mair L. O., Chowdhury S., Paredes-Juarez G. A., Guix M., Bi C., Johnson B., English B. W., Jafari S., Baker-McKee J., Watson-Daniels J., Hale O., Stepanov P., Sun D., Baker Z., Ropp C., Raval S. B., Arifin D. R., Bulte, J. W. M., Weinberg I. N., Evans B. A., and Cappelleri D. J., 2019, "Magnetically aligned nanorods in alginate capsules (MANiACs): Soft matter tumbling robots for manipulation and drug delivery," Micromachines, **10**(4), p. 230.
[51] Kim J., Park H., and Yoon C., 2022, "Advances in biodegradable soft robots," Polymers, **14**(21), p. 4574.
[52] Yan X., Xu J., Zhou Q., Jin D., Vong C. I., Feng Q., Ng D. H., Bian L., and Zhang L., 2019, "Molecular cargo delivery using multicellular magnetic microswimmers," Appl. Mater. Today, **15**, pp. 242–251.
[53] Xie L., Pang X., Yan X., Dai Q., Lin H., Ye J., Cheng Y., Zhao Q., Ma X., Zhang X., Liu G., and Chen X., 2020, "Photoacoustic imaging-trackable magnetic microswimmers for pathogenic bacterial infection treatment," ACS Nano, **14**(3), pp. 2880–2893.
[54] Yan X., Zhou Q., Yu J., Xu T., Deng Y., Tang T., Feng Q., Bian L., Zhang Y., Ferreira A., and Zhang L., 2015, "Magnetite nanostructured porous hollow helical microswimmers for targeted delivery," Adv. Funct. Mater., **25**(33), pp. 5333–5342.
[55] Mushtaq, F., Chen, X., Staufert, S., Torlakcik, H., Wang, X., Hoop, M., Gerber, A., Li, X., Cai, J., Nelsona, B. J., and Pané, S., 2019, "On-the-fly catalytic degradation of organic pollutants using magneto-photoresponsive bacteria-templated microcleaners," J. Mater. Chem. A, **7**(43), pp. 24847–24856.
[56] Carlsen R. W., Edwards M. R., Zhuang J., Pacoret C., and Sitti M., 2014 "Magnetic steering control of multi-cellular bio-hybrid microswimmers," Lab Chip, **14**(19), pp. 3850–3859.
[57] Zhang Y., Zhang L., Yang L., Vong C. I., Chan K. F., Wu W. K. K., Kwong T. N. Y., Lo N. W. S., Ip M., Wong S. H., Sung J. J. Y., Chiu P. W. Y., and Zhang L., 2019, "Real-time tracking of fluorescent magnetic spore–based microrobots for remote detection of C. diff toxins," Sci. Adv., **5**(1), p. eaau9650.
[58] Lin S., Sangaj N., Razafiarison T., Zhang C., and Varghese S., 2011, "Influence of physical properties of biomaterials on cellular behavior," Pharm. Res., **28**, pp. 1422-1430.

[59] Buchroithner B., Hartmann D., Mayr S., Oh Y. J., Sivun D., Karner A., Buchegger B., Griesser T., Hinterdorfer P., Klar T. A., and Jacak J., 2020, "3D multiphoton lithography using biocompatible polymers with specific mechanical properties," Nanoscale Adv., **2**(6), pp. 2422–2428.
[60] Belqat M., Wu X., Gomez L. P. C., Malval J. P., Dominici S., Leuschel B., Spangenberg A., and Mougin K., 2021, "Tuning nanomechanical properties of microstructures made by 3D direct laser writing," Addit. Manuf., **47**, p. 102232.
[61] Wu Y., Xiang Y., Fang J., Li X., Lin Z., Dai, G., Yin J., Wei P., and Zhang D., 2019, "The influence of the stiffness of GelMA substrate on the outgrowth of PC12 cells," Biosci. Rep., **39**(1), p. BSR20181748.
[62] Marques D. R., Santos L. A. D., Schopf L. F., Fraga J. C. S. D., 2013, "Analysis of poly (lactic-co-glycolic acid)/poly (isoprene) polymeric blend for application as biomaterial," Polímeros, **23**, pp. 579–584.
[63] Jain N., Singh V. K., and Chauhan S., 2017, "A review on mechanical and water absorption properties of polyvinyl alcohol based composites/films," J. Mech. Behav. Biomed. Mater., **26**(5–6), pp. 213–222.
[64] Eshraghi S., and Das S., 2010, "Mechanical and microstructural properties of polycaprolactone scaffolds with 1-D, 2-D, and 3-D orthogonally oriented porous architectures produced by selective laser sintering," Acta Biomater., **6**(7), p. 2467.
[65] Polyetherimide, MakeItFrom.com. https://www.makeitfrom.com/material-properties/Polyetherimide-PEI. Accessed 1 March 2024.
[66] Iza M., Stoianovici G., Viora L., Grossiord J. L., and Couarraze G., 1998, "Hydrogels of poly (ethylene glycol): mechanical characterization and release of a model drug," J. Control. Release, **52**(1–2), pp. 41–51.
[67] Ikehata A., and Ushiki H., 2002, "Effect of salt on the elastic modulus of poly (N-isopropylacrylamide) gels," Polymer, **43**(7), pp. 2089–2094.
[68] Santos Rosalem G., Gonzales Torres L. A., de Las Casas E. B., Mathias F. A. S., Ruiz J. C., and Carvalho M. G. R., 2020, "Microfluidics and organ-on-a-chip technologies: A systematic review of the methods used to mimic bone marrow," PLoS One, **15**(12), p. e0243840.
[69] Zhang B., Galluzzi M., Zhou G., and Yu H., 2023, "A study of macrophage mechanical properties and functional modulation based on the Young's modulus of PLGA-PEG fibers," Biomater. Sci., **11**(1), pp. 153–161.
[70] Steager E. B., Selman Sakar M., Magee C., Kennedy M., Cowley A., and Kumar V., 2013, "Automated biomanipulation of single cells using magnetic microrobots," Int. J. Rob. Res., **32**(3), pp. 346–359.
[71] Kline T. R., Paxton W. F., Mallouk T. E., and Sen A., 2005, "Catalytic nanomotors: remote-controlled autonomous movement of striped metallic nanorods," Angew. Chem. Int. Ed. Engl., **44**(5), pp. 744–746.
[72] Peyer K. E., Zhang L., and Nelson B. J., 2013, "Bio-inspired magnetic swimming microrobots for biomedical applications," Nanoscale, **5**(4), pp. 1259–1272.
[73] Berg H. C., and Anderson R. A., 1973, "Bacteria swim by rotating their flagellar filaments," Nature, **245**(5425), pp. 380–382.
[74] Purcell E. M., 1977, "Life at low Reynolds number," Am. J. Phys., **45**(1), pp. 3–11.
[75] Bell D. J., Leutenegger S., Hammar K. M., Dong L. X., and Nelson B. J., 2007, "Flagella-like propulsion for microrobots using a nanocoil and a rotating electromagnetic field," Proceedings 2007 IEEE International Conference on Robotics and Automation, pp. 1128–1133.
[76] Zhang L., Abbott J. J., Dong L., Peyer K. E., Kratochvil B. E., Zhang H., and Nelson B. J., 2009, "Characterizing the swimming properties of artificial bacterial flagella," Nano Lett., **9**(10), pp. 3663–3667.
[77] Zhang L., Peyer K. E., Petit T., Kratochvil B. E., and Nelson B. J., 2010, "Motion control of artificial bacterial flagella," 10th IEEE International Conference on Nanotechnology, pp. 893–896.
[78] Zhang L., Abbott J. J., Dong L., Kratochvil B. E., Bell D., and Nelson B. J., 2009, "Artificial bacterial flagella: Fabrication and magnetic control," Appl. Phys. Lett., **94**(6), p. 064107.
[79] Zhang L., Peyer K. E., and Nelson B. J., 2010, "Artificial bacterial flagella for micromanipulation," Lab Chip, **10**(17), pp. 2203–2215.
[80] Ghosh A., and Fischer P., 2009, "Controlled propulsion of artificial magnetic nanostructured propellers," Nano Lett., **9**(6), pp. 2243–2245.
[81] Hwang G., Haliyo S., and Régnier S., 2010, "Remotely powered propulsion of helical nanobelts," Robot. Sci. Syst., p. 307.
[82] Hwang G., Braive R., Couraud L., Cavanna A., Abdelkarim O., Robert-Philip I., Beveratos A., Sagnes I., Haliyo S., and Régnier S., 2011, "Electro-osmotic propulsion of helical nanobelt swimmers," Int. J. Rob. Res., **30**(7), pp. 806–819.

[83] Khalil I. S., Tabak A. F., Hamed Y., Tawakol M., Klingner A., El Gohary N., Mizaikoff B., and Sitti M., 2018, "Independent actuation of two-tailed microrobots," IEEE Robot. Autom. Lett., **3**(3), pp. 1703–1710.
[84] Hamed Y., Tawakol M., El Zahar L., Klingner A., Abdennadher S., and Khalil I. S., 2018, "Realization of a soft microrobot with multiple flexible flagella," 2018 7th IEEE Int. Conf. Biomed. Robot. Biomechatron., pp. 61–66.
[85] Xu T., Gilgueng H., Nicolas A., and Stéphane R., 2013, "Modeling and swimming property characterizations of scaled-up helical microswimmers," IEEE ASME Trans. Mechatron., **19**(3), pp. 1069–1079.
[86] Ceylan H., Yasa I. C., Yasa O., Tabak A., Giltinan J., and Sitti M., 2019, "3D-printed biodegradable microswimmer for theranostic cargo delivery and release," ACS Nano, **13**(3), pp. 3353–3362.
[87] Gao W., Sattayasamitsathit S., Manesh K. M., Weihs D., Wang J., 2010, "Magnetically powered flexible metal nanowire motors," J. Am. Chem. Soc., **132**(41), 14403–14405.
[88] Pak O. S., Gao W., Wang J., and Lauga E., 2011, "High-speed propulsion of flexible nanowire motors: Theory and experiments," Soft Matter, **7**(18), pp. 8169–8181.
[89] Dreyfus R., Baudry J., Roper M. L., Fermigier M., Stone H. A., and Bibette J., 2005, "Microscopic artificial swimmers," Nature, **437**(7060), pp. 862–865.
[90] Ludwig W., 1930, "Zur Theorie der Flimmerbewegung (Dynamik, Nutzeffekt, Energiebilanz)," J. Comp. Physiol. A Neuroethol. Sens. Neural. Behav. Physiol., **13**(3), pp. 397–504.
[91] Shah A. S., Ben-Shahar Y., Moninger T. O., Kline J. N., and Welsh M. J., 2009, "Motile cilia of human airway epithelia are chemosensory," Science, **325**(5944), pp. 1131–1134.
[92] Kim S., Lee S., Lee J., Nelson B. J., Zhang L., and Choi H., 2016, "Fabrication and manipulation of ciliary microrobots with non-reciprocal magnetic actuation," Sci. Rep., **6**(1), p. 30713.
[93] Ghanbari A., and Bahrami M., 2011, "A novel swimming microrobot based on artificial cilia for biomedical applications," J. Intell. Robot. Syst., **63**, pp. 399–416.
[94] Li, T., Li, J., Zhang H., Chang X., Song W., Hu Y., Wang J., 2016, "Magnetically propelled fish-like nanoswimmers," Small, **12**(44), pp. 6098–6105.
[95] Dodampegama S., Mudugamuwa A., Konara M., Perera N., De Silva D., Roshan U., and Tamura H., 2022, "A review on the motion of magnetically actuated bio-inspired microrobots," Appl. Sci., **12**(22), p. 11542.
[96] Xing, L., Liao, P., Mo, H., Li, D., and Sun, D., 2021, "Preformation characterization of a torque-driven magnetic microswimmer with multi-segment structure," IEEE Access, **9**, pp. 29279-29292.
[97] Qiu T., Lee T. C., Mark A. G., Morozov K. I., Münster R., Mierka O., and Fischer P., 2014, "Swimming by reciprocal motion at low Reynolds number," Nat. Commun., **5**(1), p. 5119.
[98] Palagi, S., and Fischer, P., 2018, "Bioinspired microrobots," Nat. Rev. Mater., **3**(6), pp. 113–124.
[99] Ng, C. S. X., Tan, M. W. M., Xu, C., Yang, Z., Lee, P. S., and Lum, G. Z., 2021, "Locomotion of miniature soft robots," Adv. Mater., **33**(19), p. 2003558.
[100] Hussein, H., Damdam, A., Ren, L., Obeid Charrouf, Y., Challita, J., Zwain, M., and Fariborzi, H., 2023, "Actuation of mobile microbots: a review," Adv. Intell. Syst., **5**(9), p. 2300168.
[101] Wang, X., Hu, C., Pané, S., and Nelson, B. J., 2021, "Dynamic modeling of magnetic helical microrobots," IEEE Robot. Autom. Lett., **7**(2), pp. 1682–1688.
[102] Huang, H. W., Uslu, F. E., Katsamba, P., Lauga, E., Sakar, M. S., and Nelson, B. J., 2019, "Adaptive locomotion of artificial microswimmers," Sci. Adv., **5**(1), p. eaau1532.
[103] Huang, T. Y., Sakar, M. S., Mao, A., Petruska, A. J., Qiu, F., Chen, X. B., Kennedy, S., Mooney, D. and Nelson, B. J., 2015, "3D printed microtransporters: Compound micromachines for spatiotemporally controlled delivery of therapeutic agents," Adv. Mater., **27**(42), pp. 6644–6650.
[104] Huang, T. Y., Qiu, F., Tung, H. W., Peyer, K. E., Shamsudhin, N., Pokki, J., Zhang, L., Chen, X. B., Nelson, B. J. and Sakar, M. S., 2014, "Cooperative manipulation and transport of microobjects using multiple helical microcarriers," RSC Adv., **4**(51), pp.26771–26776.
[105] Dong, X. and Sitti, M., 2020, "Controlling two-dimensional collective formation and cooperative behavior of magnetic microrobot swarms," Int. J. Rob. Res., **39**(5), pp. 617–638.
[106] Xie, H., Sun, M., Fan, X., Lin, Z., Chen, W., Wang, L., Dong, L. and He, Q., 2019, "Reconfigurable magnetic microrobot swarm: Multimode transformation, locomotion, and manipulation," Sci. Robot., **4**(28), p. eaav8006.
[107] Behrens, M. R. and Ruder, W. C., 2022, "Smart magnetic microrobots learn to swim with deep reinforcement learning," Adv. Intell. Syst., **4**(10), p. 2200023.
[108] Hou, Y., Wang, H., Fu, R., Wang, X., Yu, J., Zhang, S., Huang, Q., Sun, Y. and Fukuda, T., 2023, "A review on microrobots driven by optical and magnetic fields," Lab Chip, **23**(5), pp. 848–868.
[109] Pironneau, O., 1973, "On optimum profiles in Stokes flow," J. Fluid. Mech., **59**(1), pp. 117–128.

[110] Bourot, J. M., 1974, "On the numerical computation of the optimum profile in Stokes flow," J. Fluid. Mech., **65**(3), pp. 513–515.
[111] Diller, E. and Sitti, M., 2014, "Three-dimensional programmable assembly by untethered magnetic robotic micro-grippers," Adv. Funct. Mater., **24**(28), pp. 4397–4404.
[112] Wang, Q., Chan, K. F., Schweizer, K., Du, X., Jin, D., Yu, S. C. H., Nelson, B. J. and Zhang, L., 2021, "Ultrasound Doppler-guided real-time navigation of a magnetic microswarm for active endovascular delivery," Sci. Adv., **7**(9), p. eabe5914.
[113] Kummer, M. P., Abbott, J. J., Kratochvil, B. E., Borer, R., Sengul, A., and Nelson, B. J., 2010, "OctoMag: An electromagnetic system for 5-DOF wireless micromanipulation," IEEE Trans. Rob., **26**(6), pp. 1006–1017.
[114] Erni, S., Schürle, S., Fakhraee, A., Kratochvil, B. E., and Nelson, B. J., 2013, "Comparison, optimization, and limitations of magnetic manipulation systems," J. Microbio Robot., **8**, pp. 107–120.
[115] Petruska, A. J., 2020, "Open-loop orientation control using dynamic magnetic fields," IEEE Robot. Autom. Lett., **5**(4), pp. 5472–5476.
[116] Sitt, A., Soukupova, J., Miller, D., Verdi, D., Zboril, R., Hess, H., and Lahann, J., 2016, "Microscale rockets and picoliter containers engineered from electrospun polymeric microtubes," Small, **12**(11), pp. 1432–1439.
[117] Wang, D., Zhao, G., Chen, C., Zhang, H., Duan, R., Zhang, D., Li, M., and Dong, B., 2019, "One-step fabrication of dual optically/magnetically modulated walnut-like micromotor," Langmuir, **35**(7), pp. 2801–2807.
[118] Su, Y., Qiu, T., Song, W., Han, X., Sun, M., Wang, Z., Xie, H., Dong, M., and Chen, M., 2021, "Melt electrospinning writing of magnetic microrobots," Adv. Sci., **8**(3), p. 2003177.
[119] Tan, L., and Cappelleri, D. J., 2023, "Design, fabrication, and characterization of a helical adaptive multi-material microrobot (HAMMR)," IEEE Robot. Autom. Lett., **8**(3), pp. 1723–1730.
[120] Wei T., Liu J., Li D., Chen S., Zhang Y., Li J., and Sun D., 2020, "Development of magnet-driven and image-guided degradable microrobots for the precise delivery of engineered stem cells for cancer therapy," Small, **16**(41), p. 1906908.
[121] Limberg D. K., Kang J. H., and Hayward R. C., 2022, "Triplet–triplet annihilation photopolymerization for high-resolution 3D printing," J. Am. Chem. Soc., **144**(12), pp. 5226–5232.
[122] Bozuyuk U., Yasa O., Yasa C., Ceylan H., Kizilel S., and Sitti M., 2018, "Light-triggered drug release from 3D-printed magnetic chitosan microswimmers," ACS Nano, **12**(9), pp. 9617–9625.
[123] Ussia M., Urso M., Kratochvilova M., Navratil J., Balvan J., Mayorga-Martinez C. C., Vyskocil J., Masarik M., Pumera M., 2023, "Magnetically driven self-degrading zinc-containing cystine microrobots for treatment of prostate cancer," Small, **19**(17), p. 2208259.
[124] Martel S., Mohammadi M., Felfoul O., Lu Z., and Pouponneau P., 2009, "Flagellated magnetotactic bacteria as controlled MRI-trackable propulsion and steering systems for medical nanorobots operating in the human microvasculature," Int. J. Rob. Res., **28**(4), pp. 571–582.
[125]Magdanz V., Sanchez S., and Schmidt O., 2013, "Development of a sperm-flagella driven micro-bio-robot," Adv. Mater., **25**(45), pp. 6581–6588.
[126] Yasa O., Erkoc P., Alapan Y., and Sitti M., 2018, "Microalga-powered microswimmers toward active cargo delivery," Adv. Mater., **30**(45), p. 1804130.
[127] Hawkeye, M. M., and Brett, M. J., 2007, "Glancing angle deposition: Fabrication, properties, and applications of micro-and nanostructured thin films," J. Vac. Sci. Technol. A, **25**(5), pp. 1317–1335.
[128] Brett, M. J., and Hawkeye, M. M., 2008, "New materials at a glance," Science, **319**(5867), pp. 1192–1193.
[129] Kadiri, V. M., Bussi, C., Holle, A. W., Son, K., Kwon, H., Schütz, G., Gutierrez, M. G., and Fischer, P., 2020, "Biocompatible magnetic micro-and nanodevices: fabrication of FePt nanopropellers and cell transfection," Adv. Mater., **32**(25), p. 2001114.
[130] Walker, D., Käsdorf, B. T., Jeong, H. H., Lieleg, O., and Fischer, P., 2015, "Enzymatically active biomimetic micropropellers for the penetration of mucin gels," Sci. Adv., **1**(11), p. e1500501.
[131] Wu, Z., Troll, J., Jeong, H. H., Wei, Q., Stang, M., Ziemssen, F., Wang, Z., Dong, M., Schnichels, S., Qiu, T., and Fischer, P., 2018, "A swarm of slippery micropropellers penetrates the vitreous body of the eye," Sci. Adv., **4**(11), p. eaat4388.
[132] Schamel, D., Mark, A. G., Gibbs, J. G., Miksch, C., Morozov, K. I., Leshansky, A. M., and Fischer, P., 2014, "Nanopropellers and their actuation in complex viscoelastic media," ACS Nano, **8**(9), pp. 8794–8801.
[133] Ghosh, A., Paria, D., Rangarajan, G., and Ghosh, A., 2014, "Velocity fluctuations in helical propulsion: How small can a propeller be," J. Phys. Chem. Lett., **5**(1), pp. 62–68.

[134] Liu, L., Yoo, S. H., Lee, S. A., and Park, S., 2011, "Wet-chemical synthesis of palladium nanosprings," Nano Lett., **11**(9), pp. 3979–3982.
[135] Li, J., Sattayasamitsathit, S., Dong, R., Gao, W., Tam, R., Feng, X., Ai, S., and Wang, J., 2014, "Template electrosynthesis of tailored-made helical nanoswimmers," Nanoscale, **6**(16), pp. 9415–9420.
[136] Hoop, M., Shen, Y., Chen, X. Z., Mushtaq, F., Iuliano, L. M., Sakar, M. S., Petruska, A., Loessner, M. J., Nelson, B. J., and Pané, S., 2016, "Magnetically driven silver-coated nanocoils for efficient bacterial contact killing," Adv. Funct. Mater., **26**(7), pp. 1063–1069.
[137] Li, J., Angsantikul, P., Liu, W., Esteban-Fernández de Ávila, B., Chang, X., Sandraz, E., Liang, Y., Zhu, S., Zhang, Y., Chen, C., Gao, W., Zhang, L., and Wang, J., 2018, "Biomimetic platelet-camouflaged nanorobots for binding and isolation of biological threats," Adv. Mater., **30**(2), p. 1704800.
[138] Chen, X. Z., Hoop, M., Shamsudhin, N., Huang, T., Özkale, B., Li, Q., Siringil, E., Mushtaq, F., Tizio, L. D., Nelson, B. J., and Pané, S., 2017, "Hybrid magnetoelectric nanowires for nanorobotic applications: fabrication, magnetoelectric coupling, and magnetically assisted in vitro targeted drug delivery," Adv. Mater., **29**(8), p. 1605458.
[139] Jang, B., Hong, A., Alcantara, C., Chatzipirpiridis, G., Marti, X., Pellicer, E., Sort, J., Harduf, Y., Or, Y., Nelson, B. J., and Pané, S., 2019, "Programmable locomotion mechanisms of nanowires with semihard magnetic properties near a surface boundary," ACS Appl. Mater. Interfaces, **11**(3), pp. 3214–3223.
[140] Zhang, J., Agramunt-Puig, S., Del-Valle, N., Navau, C., Baro, M. D., Estrade, S., Peiró, F., Pané, S. Nelson, B. J., Sanchez, A. Nogués, J., Pellicer, E. and Sort, J., 2016, "Tailoring staircase-like hysteresis loops in electrodeposited trisegmented magnetic nanowires: A strategy toward minimization of interwire interactions," ACS Appl. Mater. Interfaces, **8**(6), pp. 4109–4117.
[141] Mushtaq, F., Asani, A., Hoop, M., Chen, X. Z., Ahmed, D., Nelson, B. J., and Pané, S., 2016, "Highly efficient coaxial TiO_2-PtPd Tubular nanomachines for photocatalytic water purification with multiple locomotion strategies," Adv. Funct. Mater., **26**(38), pp. 6995–7002.
[142] Ji, F., Li, T., Yu, S., Wu, Z., and Zhang, L., 2021, "Propulsion gait analysis and fluidic trapping of swinging flexible nanomotors," ACS Nano, **15**(3), pp. 5118–5128.
[143] Li, T., Li, J., Morozov, K. I., Wu, Z., Xu, T., Rozen, I., Leshansky, A. M., Li, L., and Wang, J., 2017, "Highly efficient freestyle magnetic nanoswimmer," Nano Lett., **17**(8), pp. 5092–5098.
[144] Wu, J., Jang, B., Harduf, Y., Chapnik, Z., Avci, Ö. B., Chen, X., Puigmartí-Luis, J., Ergeneman, O., Nelson, B. J., Or, Y., Pané, S., 2021, "Helical klinotactic locomotion of two-link nanoswimmers with dual-function drug-loaded soft polysaccharide hinges," Adv. Sci., **8**(8), p. 2004458.